Kinetic Behavior of Photo-Polymerization of UV-Curable Resins with Carboxylic Acid and Amino Groups

Kuo-Huai Kuo,[1] Wen-Yen Chiu,[1,2,3] Trong-Ming Don[4]

[1]*Department of Chemical Engineering, National Taiwan University, Taipei, 106 Taiwan, Republic of China*
[2]*Institute of Polymer Science and Engineering, National Taiwan University, Taipei, 106 Taiwan, Republic of China*
[3]*Department of Materials Science and Engineering, National Taiwan University, Taipei, 106 Taiwan, Province of China*
[4]*Department of Chemical and Materials Engineering, Tamkang University, Taipei, 251 Taiwan, Republic of China*

Received 20 December 2008; accepted 27 July 2009
DOI 10.1002/app.31279
Published online 7 October 2009 in Wiley InterScience (www.interscience.wiley.com).

ABSTRACT: Photo-polymerization behaviors of bisphenol-A epoxy diacrylate (EPA) and six kinds of EPA-derived resins containing different amounts of carboxylic acid, urethane, amide, and imide groups were studied by a photo differential scanning calorimetry. The dark polymerization was performed and pseudo-steady state assumption of growing radicals was made to obtain the kinetic constants for propagation, bimolecular termination, monomolecular termination, and the concentration of growing radicals of different resins as a function of extent of reaction. Compared with EPA, it was found that the rate of polymerization and kinetic constants of the six resins were relatively small because the mobility of reacting species in resins was restricted by carboxylic acid, urethane, amide, and imide groups. Finally, three different photo-initiators were used to initiate the polymerization, and their kinetic behaviors were compared. The effect of tertiary amine group of photo-initiator on the rate of polymerization of resins having carboxylic acid group and the initiator efficiency were discussed. © 2009 Wiley Periodicals, Inc. J Appl Polym Sci 115: 1982–1994, 2010

Key words: kinetic behavior; photo-polymerization; UV-curable resins

INTRODUCTION

Photo-polymerization of multifunctional monomers, oligomers, and polymers has attracted a lot of attention due to their great reactivities. They are widely used in various industries, such as protective and decorative coatings, photo-resists, orthopedic biomaterials, and dental restoration applications.[1–3] In recent years, the kinetics of photo-polymerizations of various types of multifunctional (meth)acrylates has been widely investigated in many studies. It was found that the rate of polymerization (R_p) increased rapidly at the beginning of polymerization, reached a maximum, and then decreased with time. It was because the viscosity of reaction medium increased with conversion due to the increase in molecular weight and the restricted mobility of cross-linked polymer,[4–9] therefore, the kinetic constant became conversion-dependent which resulted in different R_p upon irradiation.

Mateo et al.[8] investigated the kinetic behavior of photo-polymerization of ethylene glycol dimethacrylate. They found that the kinetic constants, such as propagation rate constant (k_p) and bimolecular termination rate constant (k_t^b), decreased with double-bond conversion, especially at a high double-bond conversion, indicating that the kinetic behavior was strongly influenced by the viscosity of reaction medium. Andrzejewska et al.[6,7] reported the photo-polymerization of triethylene glycol dimethacrylate. They found that the termination reaction occurred by both bimolecular and monomolecular terminations. They also found that the k_t^b/k_p ratio decreased from the beginning of polymerization and then with a tendency to a plateau value due to the decrease in mobility of growing radicals during polymerization.

Several kinds of multifunctional (meth)acrylates having polar functional groups such as carboxylic acid (COOH) group have been developed which is to be applied in some specific fields such as micro image in optoelectronic industry.[10–12] For example, Nishikubo and coworkers[11] disclosed a hyperbranched polyimide methacrylate containing a COOH group at the chain ends, which could be used in the negative photo-resist application. Decker et al.[13] synthesized several types of waterbased urethane acrylates also containing a COOH group. This kind of waterbased urethane acrylate could replace the role of toxic acrylic monomer diluent in coating applications due to their environment-friendly properties. However, the polar functional groups in multifunctional acrylate would affect the curing rate of polymerization. Decker and coworkers[13] found that the final double-bond conversion decreased as the concentration of COOH in urethane acrylate

Correspondence to: W.-Y. Chiu (ycchiu@ntu.edu.tw).

increased. In addition, Cook[14] investigated the influence of molecular structure on the final conversion and he found that the curing extent of bisphenol-A based dimethacrylate oligomer (bis-GMA) having a hydroxyl group was generally lower than that of the identical oligomer yet without the hydroxyl group (diethoxylated bisphenol-A dimethacrylate). It was because the mobility of the bis-GMA was restricted by hydrogen bonding from hydroxyl groups, leading to a reduced value of final double-bond conversion.

This study is focused on the influence of different functional groups such as carboxylic acid and amino groups in the reaction system on the kinetic behavior of photo-polymerization because they were less discussed in literatures. Several kinds of resins containing different amounts of carboxylic acid, urethane, amide, and imide groups were prepared from a starting material, bisphenol-A epoxy diacrylate (EPA). These EPA-derived resins are practical for commercial applications, such as carbon black-containing photo-resists in the application of liquid crystal display industry.[15,16] The R_ps of these different resins were monitored by a photo differential scanning calorimeter. The individual kinetic constants for propagation, bimolecular termination, monomolecular termination (k_t^m), and concentration of growing radicals ($[P_n^*]$) were also estimated to compare the effects of different functional groups on the kinetic behavior of resins. Furthermore, three different photo-initiators (PIs) were used and the influences of tertiary amine of PI on the initiator efficiency (f), concentration of growing radicals, and rate of polymerization were also discussed in depth.

REACTION MECHANISM AND KINETIC ANALYSIS

Principal reactions

The principal reactions of photo-polymerization of UV-curable resin initiated by a Norrish-Type I photo-initiator are listed in the following reactions (a)–(d).

(a) Initiation:

$$\mathrm{PI} \xrightarrow{\mathrm{UV}} 2\mathrm{R}^*$$
$$\mathrm{R}^* + \mathrm{M} \rightharpoonup \mathrm{P}_1^*$$

(b) Propagation:

$$\mathrm{P}_n^* + \mathrm{M} \xrightarrow{k_p} \mathrm{P}_{n+1}^*$$

(c) Bimolecular termination:

$$\mathrm{P}_n^* + \mathrm{P}_m^* \xrightarrow{k_t^b} \mathrm{P}_{n+m}$$

(d) Monomolecular termination:

(1) Radical-transfer reaction to aromatic ring of resin

$$\mathrm{P}_n^* + \mathrm{Ar-H} \xrightarrow{k_{Rtr}} \mathrm{P_nH} + \mathrm{Ar}^*$$

(2) Radical-trapped reaction by the polymer network

$$\mathrm{P}_n^* \xrightarrow{k_{trap}} (\mathrm{P}_n^*)_{\mathrm{trapped}}$$

where PI is the photo-initiator, R* is a primary radical, M is the species containing C=C, P_1^*, P_n^*, and P_m^* are growing radicals, P_{n+m} is a dead polymer from bimolecular termination, P_nH is a dead polymer produced by radical-transfer reaction to aromatic ring of resin, Ar-H is an aromatic ring of the resin, Ar* is an inactive phenyl radical on the main chain of resin, and $(P_n^*)_{\mathrm{trapped}}$ is an inactive radical trapped by the polymer network.

The polymerization is started by the dissociation of PI upon UV irradiation to produce two primary radicals, R*. The dissociation rate of PI is assumed to decay exponentially during UV irradiation. Only a portion of primary radicals from PI can react with a C=C to form a growing radical P_1^*, as described by an initiator efficiency; and the polymerization can take place through the propagation reaction of C=C to growing radicals. The propagation rate constant k_p is nearly a constant from the beginning to a certain extent of reaction. After that, the reaction medium becomes so viscous that the reaction turns out to be diffusion-controlled and the k_p value then drops off substantially with conversion. This drop of k_p results in a decrease in rate, i.e., auto-deceleration effect.[9,17,18]

Radical termination reactions also occur. In most cases, only bimolecular termination reaction [reaction (c)] is considered as a linear free-radical polymerization. However, in a crosslinking free-radical polymerization system, both bimolecular and monomolecular termination reactions are thought to be important.[4–7] The bimolecular termination occurs between two growing radicals. In multifunctional (meth)acrylate systems, the k_t^b is conversion-dependent, but the relationship is more complex than that between k_p and conversion.[9,17,18] At the beginning of polymerization, k_t^b changes from chemical control to segmental diffusion control as the polymeric network forms. This effect leads to a decrease in k_t^b, an increase in the population of growing radicals, and a

corresponding increase in the rate of polymerization, i.e., auto-acceleration effect. As the polymerization proceeds, k_t^b still decreases but its decreasing rate is not as large as that in the auto-acceleration region. At this stage, growing radicals would be in a more restricted environment and have difficulties to move toward to each other for termination. Instead, the growing radical can propagate through unreacted double bond until encountering another growing radical to terminate. This kind of termination is labeled as reaction-diffusion controlled termination and k_t^b is almost proportional to $k_p[M]$, where $[M]$ is the corresponding concentration of double bond.[6–9,17,19] As the polymerization proceeds further, a decrease in k_t^b with conversion is still observed due to the drop of k_p.

Two kinds of monomolecular termination reactions are considered: radical-transfer reaction to the aromatic ring [reaction (d)-1][4,5,20,21] because the resins used in this study all have aromatic group, and radical-trapped reaction by the polymer network [reaction (d)-2].[6,7,22] Since the growing radical becomes less and less mobile with an increase in crosslinking density during polymerization, radical-transfer reaction to aromatic ring is hindered and its rate constant, $k_{R\mathrm{tr}}$, would decrease with conversion. On the other hand, another monomolecular termination reaction, radical-trapped reaction by the polymer network, becomes more and more important and the rate constant, k_{trap}, would increase as polymerization proceeds because the growing radical becomes less and less mobile, indicating more and more growing radicals are frozen in the polymer network.

To obtain individual kinetic constants for propagation, bimolecular termination, and monomolecular termination (including radical-transfer reaction and radical-trapped reaction) as a function of extent of reaction, a series of dark polymerization experiments was performed in this study. In these experiments, the UV light source was extinguished at a given time, and the polymerization rate in the dark was still monitored by the photo-DSC. The decrease in rate was observed until the polymerization almost stopped.

As mentioned earlier, the termination process was considered as the simultaneous occurrence of bimolecular and monomolecular termination reactions. The monomolecular termination reaction constant comprises k_{trap} and $k_{R\mathrm{tr}}$[Ar-H], but they can not be separated by the dark polymerization method. For simplification, $k_{\mathrm{trap}} + k_{R\mathrm{tr}}$[Ar-H], is replaced by k_t^m, in which [Ar-H] is assumed to remain constant during polymerization. Therefore, in the absence of initiation, i.e., in the dark period, the kinetic equations for growing radicals and rate of polymerization are described below:

$$\frac{d[P_n^*]_d}{dt} = -k_t^m[\mathrm{P_n^*}]_d - 2k_t^b[\mathrm{P_n^*}]_d^2 \quad (1)$$

$$R_p = -\frac{dx}{dt} = k_p(1-x)[\mathrm{P_n^*}]_d \quad (2)$$

Assuming k_p, k_t^b, and k_t^m are approximately constant during the dark polymerization period, $[\mathrm{P_n^*}]_d$ (the instantaneous growing radical concentration in the dark period) can therefore be obtained by a direct integration of eq. (1)

$$\frac{[\mathrm{P_n^*}]_\mathrm{d}}{[\mathrm{P_n^*}]_{\mathrm{d},0}} = \frac{1}{\left(\frac{2k_t^b[\mathrm{P_n^*}]_{d,0}}{k_t^m} + 1\right)e^{k_t^m t} - \frac{2k_t^b[\mathrm{P_n^*}]_{d,0}}{k_t^m}} \quad (3)$$

where t is the time from the start of dark polymerization and $[\mathrm{P_n^*}]_{d,0}$ is the growing radical concentration at the time of closing the shutter.

Afterwards, the growing radical concentration in the dark, $[\mathrm{P_n^*}]_d$, in eq. (3) is substituted into eq. (2) to obtain the relationship of conversion with time as given in eq. (4)

$$\ln\left(\frac{1-x_0}{1-x}\right) = \frac{k_p[\mathrm{P_n^*}]_{d,0}}{2k_t^b[\mathrm{P_n^*}]_{d,0}}\ln\left(1 + \frac{2k_t^b}{k_t^m}[\mathrm{P_n^*}]_{d,0}\left(1 - e^{-k_t^m t}\right)\right) \quad (4)$$

x_0 and x are referred to the double-bond conversion at $t = 0$ and the time from the start of dark polymerization, respectively. The value of $k_p[\mathrm{P_n^*}]_{d,0}$ is calculated from the rate of polymerization divided by the value of $1 - x_0$ at the time of closing the shutter.

The following eq. (5) shows the relationship between $k_t^b[\mathrm{P_n^*}]_{d,0}$ and k_t^m obtained by setting the time to be infinite in eq. (4), in which the value of $\ln[(1 - x_0)/(1 - x)]_{t\to\infty}$ can be acquired from the experimental data.

$$\ln\left(\frac{1-x_0}{1-x}\right)_{t\to\infty} = \frac{k_p[\mathrm{P_n^*}]_{d,0}}{2k_t^b[\mathrm{P_n^*}]_{d,0}}\ln\left(1 + \frac{2k_t^b[\mathrm{P_n^*}]_{d,0}}{k_t^m}\right) \quad (5)$$

By differentiating eq. (3) with respect to time at $t = 0$, another equation relating $k_t^b[\mathrm{P_n^*}]_{d,0}$ with k_t^m can be obtained as given in eq. (6). The value of $d([\mathrm{P_n^*}]_d/[\mathrm{P_n^*}]_{d,0})/dt$ at $t = 0$ is equal to $d[(R_p/(1 - x))/(R_p/(1 - x_0))]/dt$ at $t = 0$ and it can be calculated from the experimental data.

$$\left.\frac{d\left([\mathrm{P_n^*}]_d/[\mathrm{P_n^*}]_{d,0}\right)}{dt}\right|_{t=0} = \left.\frac{d\left[\left(R_p/(1-x)\right)/\left(R_p/(1-x_0)\right)\right]}{dt}\right|_{t=0} = -\left(2k_t^b[\mathrm{P_n^*}]_{d,0} + k_t^m\right) \quad (6)$$

Substituting the relationship between $k_t^b[\mathrm{P_n^*}]_{d,0}$ and k_t^m of eq. (6) into eq. (5), the individual kinetic constants, $k_t^b[\mathrm{P_n^*}]_{d,0}$ and k_t^m, are then obtained.

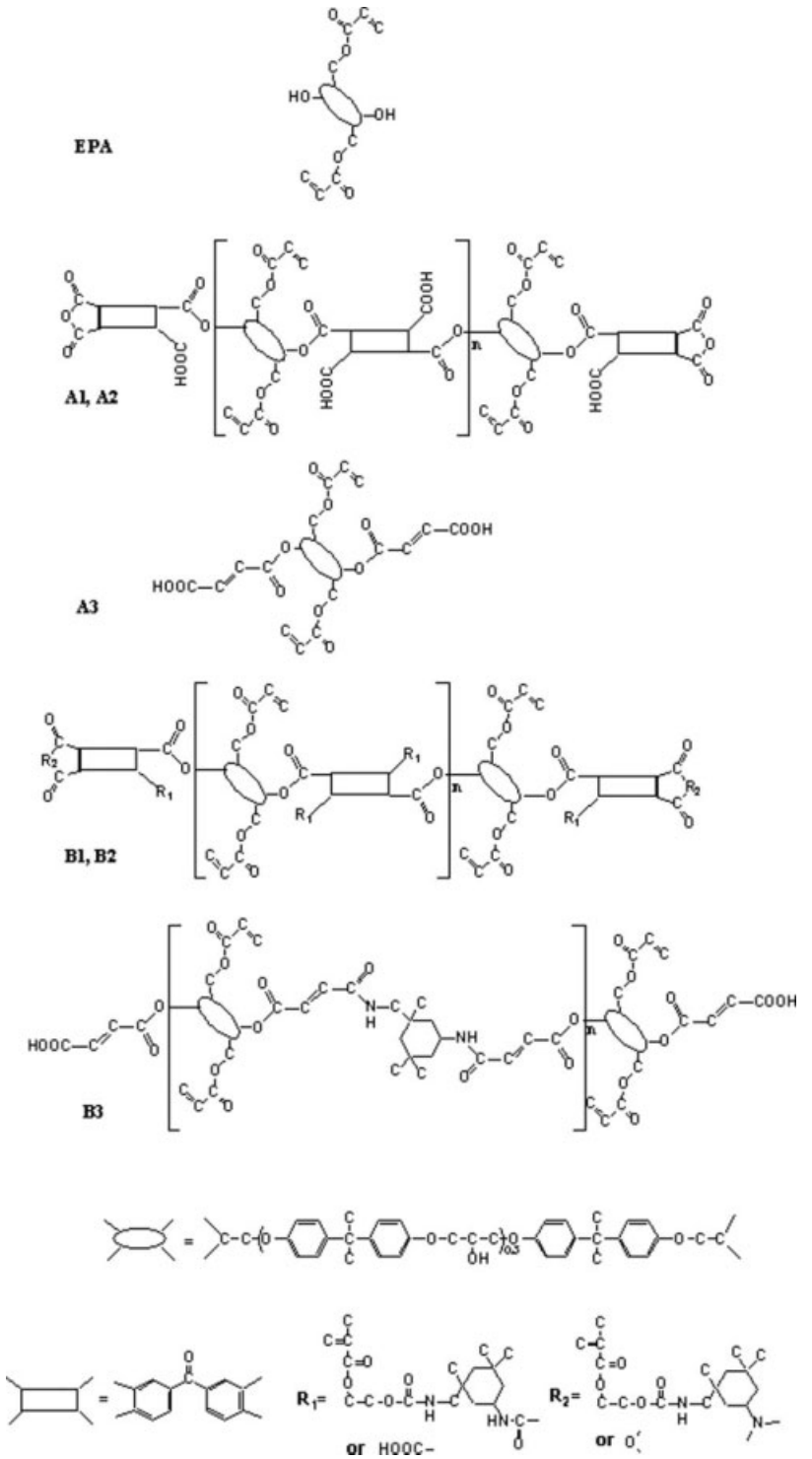

Scheme 1 Molecular structures of EPA, A1, A2, A3, B1, B2, and B3.

According to the pseudo-steady-state assumption of growing radicals at the time of closing the shutter shown in eq. (7), $[P_n^*]_{d,0}$ can be calculated from the rate of initiation divided by the value of $(2k_t^b[P_n^*]_{d,0} + k_t^m)$ as shown in eq. (8).

$$R_i - k_t^m[P_n^*]_{d,0} - 2k_t^b[P_n^*]_{d,0}^2 = 0 \quad (7)$$

$$[P_n^*]_{d,0} = \frac{R_i}{2k_t^b[P_n^*]_{d,0} + k_t^m} \quad (8)$$

Where R_i is the rate of initiation, and it is equal to $2fk_d[I]_0\exp(-k_dt)$. k_d is the decomposition rate constant of PI, f is the initiator efficiency, $[I]_0$ is the concentration of PI before UV irradiation, and t is the reaction time during irradiation. Afterwards, the

individual kinetic rate constants, k_p and k_t^b, with different extent of reaction are then calculated from the values of $k_p[P_n^*]_{d,0}$ and $k_t^b[P_n^*]_{d,0}$ divided by $[P_n^*]_{d,0}$.

EXPERIMENTAL

Materials and methods

Bisphenol-A epoxy diacrylate (EPA, AGI) and six kinds of alkali-soluble resins were prepared to investigate the effect of functional groups on the photopolymerization. The procedures to synthesize alkali-soluble resins were described elsewhere,[15,16] but their structures and concentrations of functional groups are listed in Scheme 1 and Table I, respectively. The rate of polymerization of resin was determined by a photo-DSC (Perkin–Elmer Diamond DSC coupled with EXFO OmniCure Series 2000) and the experimental procedure is described in the following:

Sample was first prepared by dissolving specific amounts of resin (10 wt %) and PI (0.1 wt %) into the solvent, propylene glycol monomethyl ether acetate (PGMEA, Grand Chemical). Several different kinds of PI were used here for comparison, namely, 2,4,6-trimethyl benzoyldiphenyl phosphine oxide (Luicirin TPO, BASF), 2-methyl-1-4-(metylthio)phenyl)-2-morpholino-propan-2-one (I907, Ciba), and 2-benzyl-2-dimethylamino-1-(4-morpholinophenyl)-butan-1-one (I369, Ciba). Approximately 30 mg of the above solution was dropped into an aluminum pan by a micro-pipette. It was then carefully placed into an oven at 50°C for 1 h to evaporate the solvent. The sample was removed from the photo-DSC, covered by a quartz glass, and equilibrated at 50°C for 10 min. Polymerization was initiated by the irradiation of UV light in a nitrogen atmosphere. The light intensity was 1.3 mW/cm^2, and the wavelength range of light is 250–450 nm. In addition to the continuous irradiation, a series of dark polymerization experiment was also carried out to obtain individual kinetic constants. In these experiments, light was extinguished by closing the shutter after a certain time of UV irradiation, and the heat of polymerization was still monitored in the dark for 3 min.

The molar amounts of acrylate, methacrylate, and maleate double bonds per kilogram of various resins are listed in Table I. However, the heat of reaction from acrylate, methacrylate, and maleate groups of resins cannot be separated by the photo-DSC experiment; therefore, the rate of polymerization is assumed to be an average consumption rate of acrylate, methacrylate, and maleate groups. The average reaction rate can be therefore defined as follows[23,24]:

TABLE I
Functional Group Concentration of EPA, A1, A2, A3, B1, B2, and B3

Resin[a]	Components[b]	Molar ratio	Imide group (mol/kg)[c]	NH group (mol/kg)[d]	Carboxylic acid (mol/kg)[e]	Aromatic ring (mol/kg)[f]	Acrylate (mol/kg)[g]	Methacrylate (mol/kg)[h]	Maleate (mol/kg)[i]	Total amount of C=C double bond (C=C-mol/kg)[j]
EPA	EPA	1	0	0	0	5.1	3.9	0	0	3.9
A1	EPA : BTDA	1 : 2	0	0	5.1	5.7	1.7	0	0	1.7
A2	EPA : BTDA	5 : 4	0	0	2.3	5.5	2.6	0	0	2.6
A3	EPA : MA	1 : 2	0	0	3.0	3.7	2.8	0	2.8	5.6
B1	EPA : BTDA : IPDI-HEMA	1 : 2 : 2	0.7	1.6	2.2	3.7	1.1	1.1	0	2.2
B2	EPA : BTDA : IPDI-HEMA	5 : 4 : 2.67	0.2	0.9	1.5	4.5	2.1	0.6	0	2.7
B3	EPA : MA : IPDI	5 : 10 : 4	0	2.0	1.7	3.2	2.5	0	2.5	5.0

[a] A1 and A2 were synthesized through an esterification with different molar ratios of EPA to BTDA. A3 was synthesized from EPA with MA through an esterification. B1 and B2 were synthesized from A1 and A2 with different molar amounts of HEMA-IPDI monomer. B3 was synthesized from A3 with IPDI.
[b] BTDA is benzophenone tetracarboxylic dianhydride; MA is maleic anhydride; HEMA is 2-Hydroxyethyl methacrylate; IPDI is isophorone diisocyanate; HEMA-IPDI is an isocyanate-containing methacrylate monomer synthesized by an equal mole of HEMA and IPDI.
[c] Concentration of imide groups of B1 and B2 were determined by the comparison of FTIR absorption spectra before and after reactions.
[d] Concentration of NH group is calculated by subtracting concentration of imide groups from total concentration of urethane, amide, and imide groups calculated according to the composition.
[e] Concentration of COOH group was determined by a titration method.
[f] Concentration of aromatic ring is calculated from composition.
[g,h,i] Concentration of acrylate, methacrylate, and maleate groups are calculated from composition, respectively.
[j] Total amount of C=C double bond equals to the sum of acrylate, methacrylate, and maleate groups.

$$R_p = \frac{dx}{dt} = \frac{1}{\Delta H_{\text{total}}}\left(\frac{dH}{dt}\right)_T \quad (9)$$

where dx/dt (1/s) is the average rate of polymerization; x is the average double-bond conversion; t (s) is the reaction time; $(dH/dt)_T$ (kJ/s) is the heat flow at a constant temperature recorded by the photo-DSC; ΔH_{total} (kJ) is the total exothermic heat of polymerization and defined in eq. (10).

$$\Delta H_{\text{total}} = \left(\Delta H_1^0 \times n_1 + \Delta H_2^0 \times n_2 + \Delta H_3^0 \times n_3\right) \times m \quad (10)$$

where ΔH_1^0, ΔH_2^0, and ΔH_3^0 are the theoretical heat of reaction of the acrylate, methacrylate, and maleate double bond, 78, 56, and 60 kJ/mol,[25,26] respectively; n_1, n_2, and n_3 (mol/kg) are the mole of acrylate, methacrylate, and maleate double bond per kilogram of resin, respectively; m (kg) is the weight of resin in samples. The extent of reaction (reacted C=C-mol/kg) over the reaction time is thus calculated according to eq. (11).

$$\text{Extent of reaction} = \frac{(n_1 + n_2 + n_3)}{\Delta H_{\text{total}}}\int_0^t \left(\frac{dH}{dt}\right)_T dt \quad (11)$$

UV/Vis spectrometry

PI and 2,2,6,6-tetramethylpiperidinooxy (TEMPO, ACROS) were dissolved in PGMEA solution. The concentration of PI and TEMPO in PGMEA were 1.6×10^{-2} and 6.4×10^{-2} mol/kg, respectively. Approximately 3 mL of the above solution was dropped into a tissue culture dish with a diameter of 6 cm. It was then irradiated by UV light with the light intensity of 1.3 mW/cm^2 for a given time period. Afterwards, the PI/TEMPO solution was dropped into a quartz cell with a path length of 1 cm and the absorption spectrum of this solution was recorded by using an UV/Vis spectrophotometer (ThermoSpectronic HEλIOS). The PI/TEMPO solution in the cell was subjected to UV/Vis light between 350 and 700 nm. The data interval was 1.0 nm. The photolysis of PI was monitored by measuring the change in the maximum absorption peak of TEMPO.

RESULTS AND DISCUSSION

Rate of polymerization by continuous UV-irradiation

From the kinetic point of view, photo-polymerizations of multifunctional resins are very complicated due to the fast reaction rate and a rapid increase in viscosity with an increase in crosslinking density.

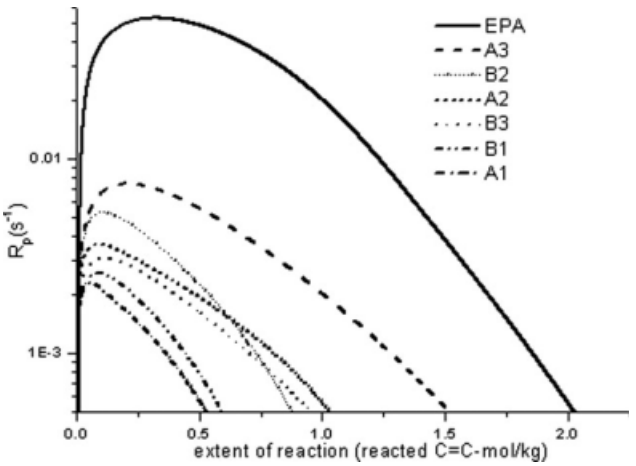

Figure 1 R_p-extent of reaction curves of different resins initiated by TPO. The intensity of UV light is 1.3 mW/cm^2 and the irradiation time is 8 min. The complete extent of reaction of each resin is listed in Table I.

Therefore, kinetic constants of multifunctional resins are extremely dependent on the mobility of reacting species.

By using the same photo-initiator TPO, Figure 1 shows the rates of polymerization versus extent of reaction of several kinds of multifunctional resins with different concentration of functional groups. For all resins, a rapid increase in R_p at the early stage of polymerization was observed. It was attributed to the decrease in termination rate which resulted from diffusion limitation of growing radicals, i.e., auto-acceleration effect. After the polymerization passed through $R_{p,\max}$, R_p kept decreasing with time. It was because the crosslinking density of reaction medium was getting higher and higher, and the mobility of growing radicals continued to decrease; which resulted in the decrease of R_p with time. Eventually, the crosslinking density was high enough to bring the reaction medium into a highly viscous state, causing the cease of reaction.

As mentioned in introduction, the polar functional groups of resin, such as hydroxyl group, can produce hydrogen bonding which reduces the mobility of reacting species and final double-bond conversion.[14] Taking EPA and A3 for examples, both EPA and A3 could produce intermolecular hydrogen bonding by hydroxyl group and COOH group, respectively, but $R_{p,\max}$ of A3 was approximately five times smaller than that of EPA, indicating that intermolecular hydrogen bonding by COOH groups was stronger than that by hydroxyl groups. Hence, the restricted mobility of A3 by stronger hydrogen bonding from COOH groups resulted in a smaller R_p.

Compared with EPA and A3, even smaller R_ps were observed for the other resins in Figure 1. Unfortunately, the structures of these resins are not

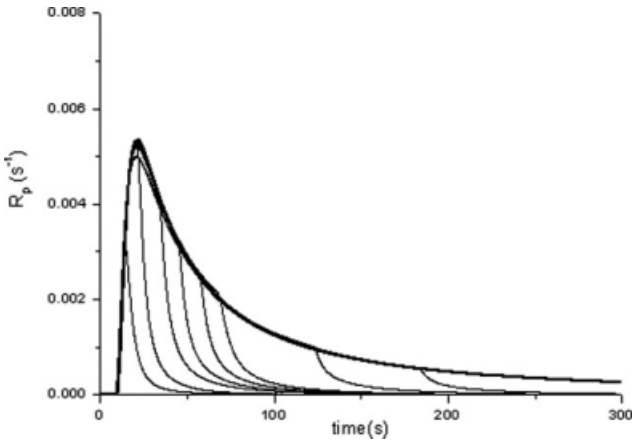

Figure 2 R_p-time curves for eight different dark polymerizations of B2 initiated by TPO. The upper curve corresponds to the polymerization during the continuous illumination.

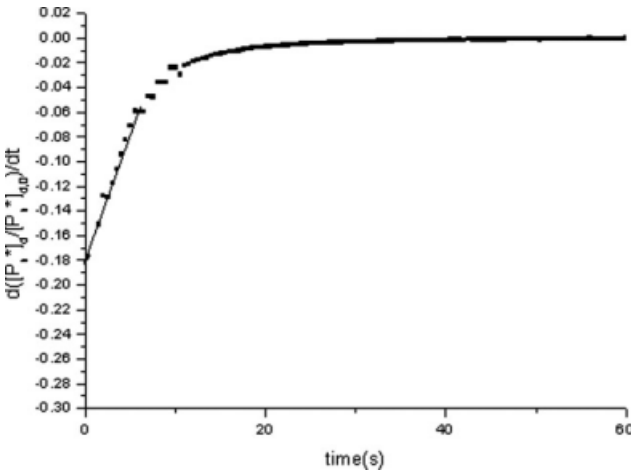

Figure 3 The $d([P_n^*]d/[P_n^*]d,0)/dt$-time curve is obtained by the differentiation of $[R_p/(1 - x)]/[R_p/(1 - x_0)]$-time curve. The value of $d([P_n^*]d/[P_n^*]d,0)/dt$ at $t = 0$ is equal to $-(k_t^b[P_n^*]d,0+k_t^m)$.

as simple as EPA and A3, because they contain not only COOH group, but also other kinds of functional groups, such as urethane, amine, and imide groups. The COOH, urethane, amine, and imide groups of these resins could produce hydrogen bonding with each other, which also limited the mobility of reacting species. Therefore, the relationship between these functional groups and R_ps could not be easily explained by R_p versus extent of reaction curve. In view of this, various kinetic rate constants of these resins were calculated by using a method which combined the dark polymerization and pseudo-steady state assumption of growing radicals to discuss the effect of different functional groups on the kinetic behavior of EPA-derived resins.

Rate of polymerization using the dark polymerization method

Figure 2 shows the representative kinetic curves of resin B2 using TPO photo-initiator in a dark polymerization method, where rate of polymerization, conversion, and extent of reaction could be calculated from these curves [cf. eqs. (9)–(11)]. The curve of $k_p[P_n^*]_{d,0}$ at the time of closing the shutter could be calculated using eq. (2). Subsequently, the ratio of the growing radical concentration in the dark at any time to that at the time of closing the shutter, $[P_n^*]_d/[P_n^*]_{d,0}$, could also be obtained. The differentiation curve of $[P_n^*]_d/[P_n^*]_{d,0}$ with time was thus calculated and shown in Figure 3. By the combination of eqs. (5) and (6), $k_t^b[P_n^*]_{d,0}$ and k_t^m values were then obtained. To separate k_p and k_t^b from $k_p[P_n^*]_{d,0}$ and $k_t^b[P_n^*]_{d,0}$, $[P_n^*]_{d,0}$ has to be known first. Therefore, according to eq. (8), R_i has to be determined to obtain all the kinetic rate constants of resins.

Norrish-Type I PIs were used in this study, which can produce radicals by the photo-cleavage mechanism. To calculate the decomposition rate constant (k_d) of PI, an efficient radical scavenger, TEMPO, was used. PI and TEMPO were mixed together and the k_d of PI was then calculated by monitoring the UV absorption peak of TEMPO during UV irradiation. As shown in Figure 4, the absorption peaks of TPO and TEMPO were at 381 and 470 nm, respectively, and they both decreased in intensity during UV irradiation. The decrease in absorbance at 470 nm is due to the consumption of TEMPO by the reaction which produced radicals from PI. On the basis of the first order kinetic assumption, the k_d can be calculated according to the following equation:

$$\ln\left(\frac{[PI]_0}{[PI]_t}\right) = \ln\left(\frac{A_0 - A_i}{A_t - A_i}\right)_{470nm} = k_d t \qquad (12)$$

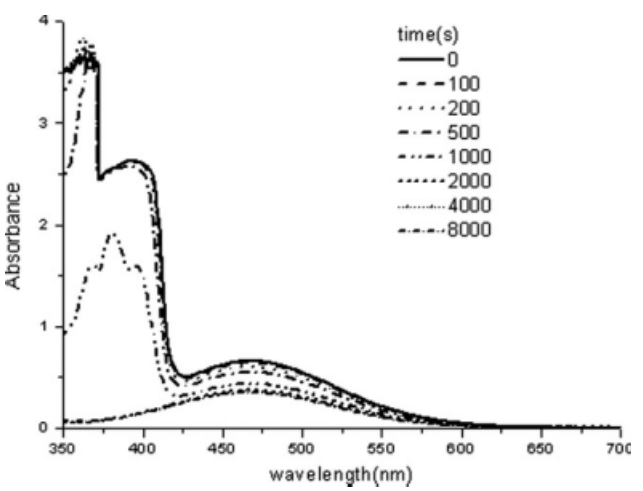

Figure 4 The absorption spectra of TPO/TEMPO mixture in PGMEA during irradiation. The intensity of UV light is 1.3 mW/cm^2.

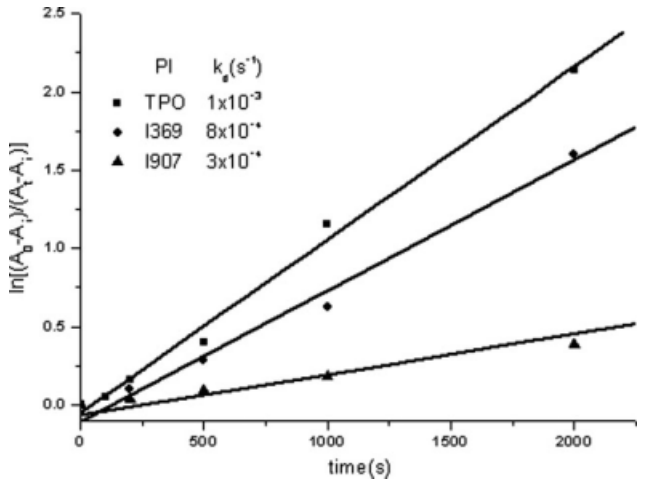

Figure 5 Linear plots of $\ln[(A_0-A_i)/(A_t-A_i)]$ versus time of TPO, I369, and I907.

where $[PI]_0$ and $[PI]_t$ denote the concentration of TPO at the exposure time of 0 and t. A_0, A_t, and A_i are the absorbances of TEMPO at 470 nm at exposure time of 0, t, and infinite time, respectively. k_ds of different PIs were then obtained from the slop of the $\ln[(A_0-A_i)/(A_t-A_i)]$ versus time as shown in Figure 5.

Besides, the initiator efficiency (f) of PI needs to be assumed to obtain R_i value. In the crosslinking polymerization system, the initiator efficiency is relatively small compared with the linear polymerization system. This is because the viscosity of the crosslinking polymerization system is relatively high, which limits the mobility of primary radicals. The resins used in this study are either highly viscous liquid or solid at room temperature, therefore, the f_{TPO} is assumed to be 0.3.[22] Once R_i is known, $[P_n^*]_{d,0}$ can be calculated according to eq. (8). Therefore, all the kinetic constants, k_p, k_t^b, and k_t^m were solved. The same procedure was applied to the other resins to obtain their kinetic constants.

Effect of different functional groups on k_p

Figure 6 shows the experimentally determined k_p values of different resins. Apparently, for all resins, the k_ps remain unchanged only for a very short period of time. As the polymerization proceeded, the reaction medium already became very viscous, and the mobility of double bond continued to decrease, therefore, k_p became diffusion-controlled and decreased significantly. Finally, the value of k_p was so small that no further reaction was observed, even though a large amount of unreacted double bonds still remained in the reaction medium.

Among all resins, the k_p of EPA was the largest because the mobility of reaction species was only limited by a weak intermolecular hydrogen bonding from hydroxyl groups. However, the k_ps of other resins were much lower than that of EPA. For instance, the k_p of A3 was about 10 times smaller than that of EPA because the mobility of A3 was strongly restricted by the intermolecular hydrogen bonding from COOH groups.

The other resins contain not only COOH group but also amino groups (urethane, amide, and imide groups), which produce hydrogen bonding.[27–29] The mobility of reacting species is thus restricted by hydrogen bonding, causing the changes of k_ps of resins. The influence of the concentration of COOH group on k_p can be discussed by the comparison between resins A1 and A2 because their molecular structures are similar. The concentration of COOH of A1 was higher than that of A2, and the k_p of A1 was smaller than that of A2. Therefore, we believe that stronger hydrogen bonding produced from higher concentration of COOH group leads to a smaller k_p value.

The influence of amino functional groups on k_p can be discussed by comparing A series with B series of resins, because B series of resins were synthesized from A series of resins with isocyanate-containing compounds to form urethane, amide, or imide group. As listed in Table I, although the concentration of COOH group of B3 was smaller than that of A3, k_p of B3 was still smaller than that of A3. It was because B3 had not only COOH group but also NH group, both of which would produce hydrogen bonding. The total concentration of COOH and NH groups of B3 was calculated as 3.7 mol/kg, larger than that of A3 (3.0 mol/kg). Therefore, we believe that the total intermolecular interaction of B3 was larger than that of A3, thus leading to a smaller k_p value for B3.

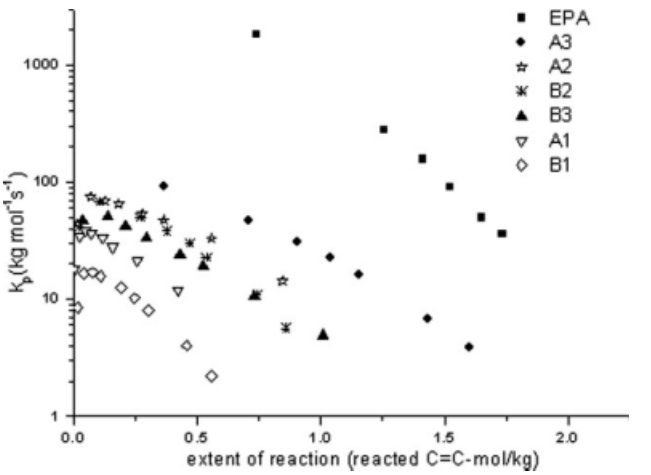

Figure 6 The relationship between k_p and the extent of reaction of different resins.

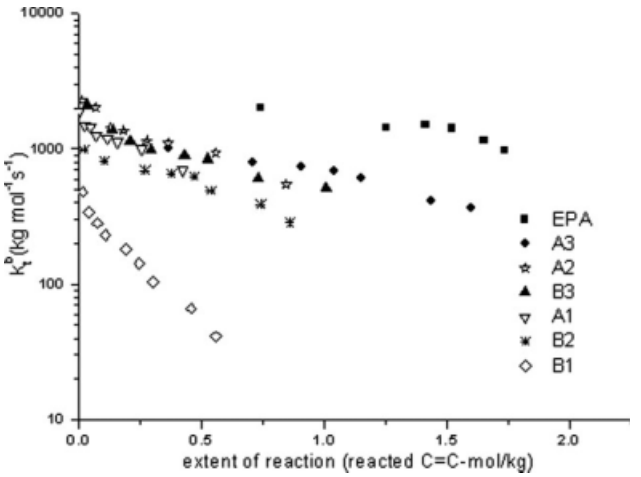

Figure 7 The relationship between k_t^b and the extent of reaction of different resins.

According to the above discussion, k_p decreases with the total concentration of COOH and NH groups. However, the k_p of B1 was smaller than that of A1 although the total concentration of COOH and NH groups of B1 (3.8 mol/kg) was smaller than that of A1 (5.1 mol/kg). As shown in Scheme 1 and Table I, B1 contained imide group at the concentration of 0.7 mol/kg which is rigid and can also form hydrogen bonding with COOH and NH groups to make the reaction species of B1 less mobile, resulting in a smaller k_p value. Besides, the smaller k_p of B2, compared with A2, was also observed, especially at higher extent of reaction. Although the total concentration of COOH and NH groups of A2 and B2 were close to each other, B2 had imide group (0.2 mol/kg), which also limits the mobility of double bond and leads to a smaller k_p.

Effect of different functional groups on k_t^b

Figure 7 shows the k_t^b values of various resins as a function of extent of reaction. For all resins, k_t^b decreased with the extent of reaction because the mobility of growing radicals decreased due to the increasing viscosity of reaction system. In general, k_t^b for small molecules such as reactive diluents largely decreases at the initial stage of polymerization as the bimolecular termination is controlled by segmental-diffusion. As the polymerization proceeds, k_t^b changes to a plateau value because the bimolecular termination becomes reaction-diffusion controlled. In contrast to the reactive diluents, no large decline in k_t^b for the resins used in this study was observed at the beginning of polymerization. Because the resins are either highly viscous liquid or solid, we believe that the bimolecular termination was dominated by reaction-diffusion controlled termination almost over the whole range of polymerization.

The effect of different functional group on k_t^b is also discussed by comparison between different resins. At the same extent of reaction, the k_t^b of EPA was the highest in all resins. It was because of its weak intermolecular hydrogen bonding from hydroxyl group, leading to a less viscous reaction system and a higher mobility of growing radicals. For the other resins, the mobility of growing radicals was largely restricted by COOH and amino groups. By the comparison between A1 and A2, it was found that the k_t^b of A1 was smaller than that of A2, indicating that k_t^b decreased as the concentration of COOH group increased. By comparing A3 with B3, it was found that the k_t^b of B3 was slightly smaller than that of A3. It was because the total concentration of COOH and NH groups of B3 was slightly larger than that of A3. Therefore, the mobility of growing radicals and k_t^b in B3 were lower because of its stronger hydrogen bonding than A3.

Another interesting behavior observed in this figure was that the k_t^b of B1 was much smaller than those of other resins. This implies that the mobility of growing radicals of B1 was extremely restricted. This is because B1 contains imide group which is rigid and can form hydrogen bonding with COOH and NH groups to cause a greater decrease in the mobility of growing radicals and k_t^b. The k_t^b of B2 was also small compared to other resins; however, it was not as small as that of B1. Since the concentration of imide group of B2 was smaller than that of B1, the mobility of growing radicals in B2 was less restricted than B1.

Effect of different functional groups on k_t^m

The monomolecular termination comprises two reactions: radical-transfer reaction to aromatic ring of resin, and radical-trapped reaction by the polymer network, therefore, the k_t^m is assumed to be equal to $k_{R\mathrm{tr}}$[Ar-H] + k_{trap}. As the polymerization proceeds, the reaction medium becomes more and more viscous, causing the growing radicals less and less mobile. This would result in a decrease in $k_{R\mathrm{tr}}$ and an increase in k_{trap} with the extent of reaction. Because these two termination reactions compete with each other, we can not forecast the trend of k_t^m with extent of reaction.

k_t^m was obtained by solving eqs. (5) and (6) according to the dark polymerization method, and the calculated k_t^m values of various resins at different extents of reaction were shown in Figure 8. Apparently, k_t^ms of all resins decreased from the beginning of polymerization, and then reached an almost unchanged value after a certain extent of reaction. As mentioned earlier, the $k_{R\mathrm{tr}}$[Ar-H] should keep

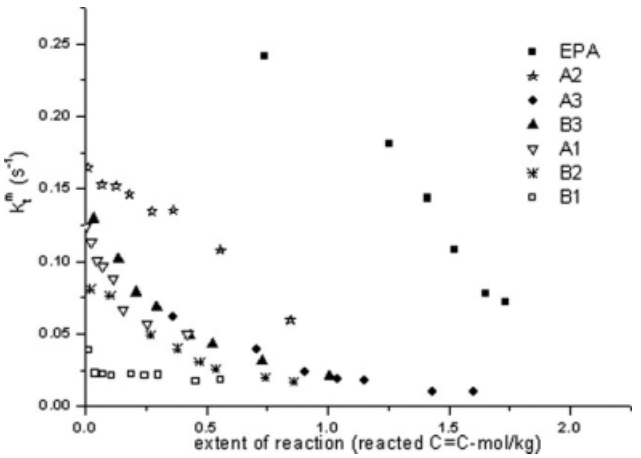

Figure 8 The relationship between k_t^m and the extent of reaction of different resins.

decreasing with polymerization because the mobility of growing radicals was restricted by the increasing viscosity in reaction medium. Therefore, we believe that the monomolecular termination at the beginning of polymerization was dominated by the radical-transfer reaction to aromatic ring of resin rather than radical-trapped reaction by the polymer network, i.e., k_t^m was almost equal to k_{Rtr}[Ar-H]. However, the value of k_t^m in Figure 8 did not keep decreasing at high extent of reaction; instead, it remained an almost constant value. Therefore, we believe that the monomolecular termination at later stage of polymerization was also influenced by another kind of monomolecular termination, radical-trapped reaction by the polymer network. At later stage of reaction, the k_{Rtr} became negligible but the viscosity was so high that k_{trap} became important and even dominated. Finally, k_t^m was almost equal to k_{trap}, and the monomolecular termination was dominated by radical-trapped reaction by the polymer network.

At the early stage of polymerization, k_t^m was dependent on the mobility of growing radicals and the concentration of aromatic ring, i.e., $k_t^m = k_{Rtr}$[Ar-H]. As shown in Figure 8, the k_t^m value of EPA was the largest in all resins. It was because the mobility of growing radicals in EPA at early stage of polymerization was high, besides, the concentration of aromatic ring was high, about 5.1 mol/kg. By contrast, the mobility of growing radicals in other resins was strongly restricted by COOH and amino groups, thus a decrease in k_t^m was observed.

The effect of the concentration of COOH group on k_{Rtr} of resin is discussed by the comparison between A1 and A2, and it was found that the k_t^m of A1 was smaller than that of A2. As listed in Table I, the concentrations of aromatic ring of these two resins were almost the same, therefore, the k_{Rtr} of A2 was larger than that of A1, indicating that k_{Rtr} was lowered with a larger concentration of COOH group.

It was found that k_t^ms of A3 and B3 were almost the same. As shown in Table I, both the total concentration of COOH and NH groups, and the concentration of aromatic ring were close for A3 and B3, resulting in a similar value of k_t^m. Figure 8 also shows that the k_t^m of B1 was the smallest in all resins. It was because the mobility of growing radicals in B1 was strongly restricted by imide group, even though the concentration of aromatic ring of B1 was not the lowest. Besides, the plateau region of k_t^m of B1 began at a relatively low extent of reaction of 0.04 (reacted C=C mol/kg), indicating that the monomolecular termination of B1 was almost dominated by radical-trapped reaction by the polymer network. This is not surprising because the mobility of growing radicals was strongly restricted by imide group. By contrast, the constant value of k_t^m of other resins, such as A3, began at a higher extent of reaction of about 1.0 (reacted C=C mol/kg). This also confirms that the mobility of growing radicals in B1 was much smaller than that of other resins.

Concentration of growing radicals during polymerization

The relationship between the concentration of growing radicals and the extent of reaction is shown in Figure 9, in which $[P_n^*]$ is equal to $[P_n^*]_{d,0}$. Apparently, the increased population of $[P_n^*]$ for all resins was observed from the starting of polymerization, because both k_t^b and k_t^m decreased as the reaction medium became more and more cross-linked. Therefore, growing radicals were terminated more and more difficultly, i.e., $[P_n^*]$ increased with the extent of reaction. The $[P_n^*]$ of EPA increased slowly and was the smallest in all resins because both k_t^b and k_t^m were the largest. On the contrary, the $[P_n^*]$ of B1 accumulated rapidly and was the largest in all

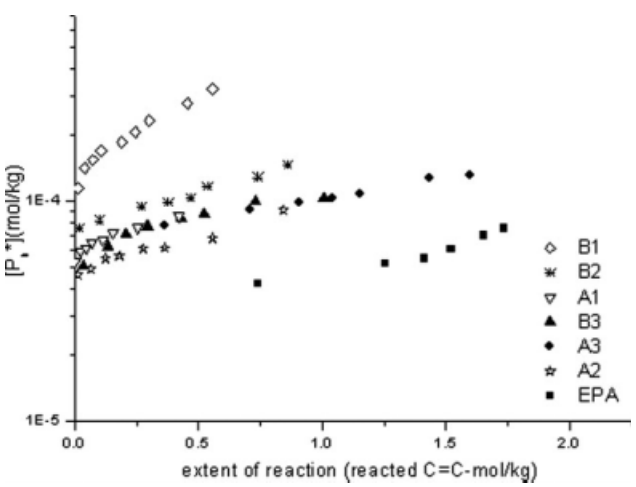

Figure 9 The relationship between $[P_n^*]$ and the extent of reaction of different resins. The PI is TPO and the intensity of UV light is 1.3 mW/cm^2.

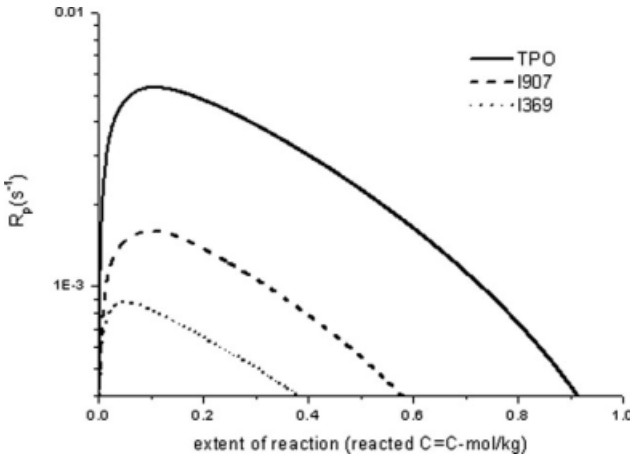

Figure 10 R_p-extent of reaction curves of B2 initiated by TPO, I369, and I907, respectively. The intensity of UV light is 1.3 mW/cm^2 and the irradiation time is 8 min.

resins, which could slightly improve rate of polymerization even though its k_p was the lowest in all resins. As the mobility of growing radicals in B1 was strongly restricted by imide group, the growing radicals thus could not be easily terminated by both monomolecular and bimolecular terminations.

Effect of tertiary amine of photo-initiator on the polymerization

In this study, photo-polymerization initiated by different PIs was also discussed. Three PIs, TPO, I907, and I369, were used to initiate the polymerization of B2. As shown in Figure 10, it was found that the R_p by TPO was the largest one in these three, and R_p decreased in the order of TPO > I907 > I369. From this result, it was expected that there should be the same trend of R_i, yet the k_d decreased in the order of TPO > I369 > I907. Although the k_ds of TPO and I369 were close, the R_p by I369 was much smaller than that by TPO. In view of this, we believe that f_{I369} was relatively small.

Because I907 and I369 contain tertiary amine group, we believe that the mobility of the generated primary radical from PI was retarded by zwitterionic interaction from the COOH of B2 and tertiary amine group of I907 and I369 (shown in Scheme 2),[30,31] which reduced the initiator efficiency and R_p. This deduction can be further confirmed by observing the concentration of growing radicals and initiator efficiency of different PIs during polymerization.

In this study, the f_{TPO} was assumed to be 0.3 and the value of $[P_n^*]$ of B2 initiated by TPO was estimated and shown in Figure 9. The f and $[P_n^*]$ for I907 and I369 can be estimated according to the procedure as follows:

The values of $[P_n^*]$ for I907 and I369 were first calculated from $k_p[P_n^*]$ divided by k_p; where $k_p[P_n^*]$ for I907 and I369 were calculated from the R_p divided by the $1 - x_t$ at the reaction time t during irradiation (Fig. 10), and k_p was taken from the curve of B2 shown in Figure 6. Because PI in reaction medium was as low as 1 wt %, the kinetic constants such as k_p,

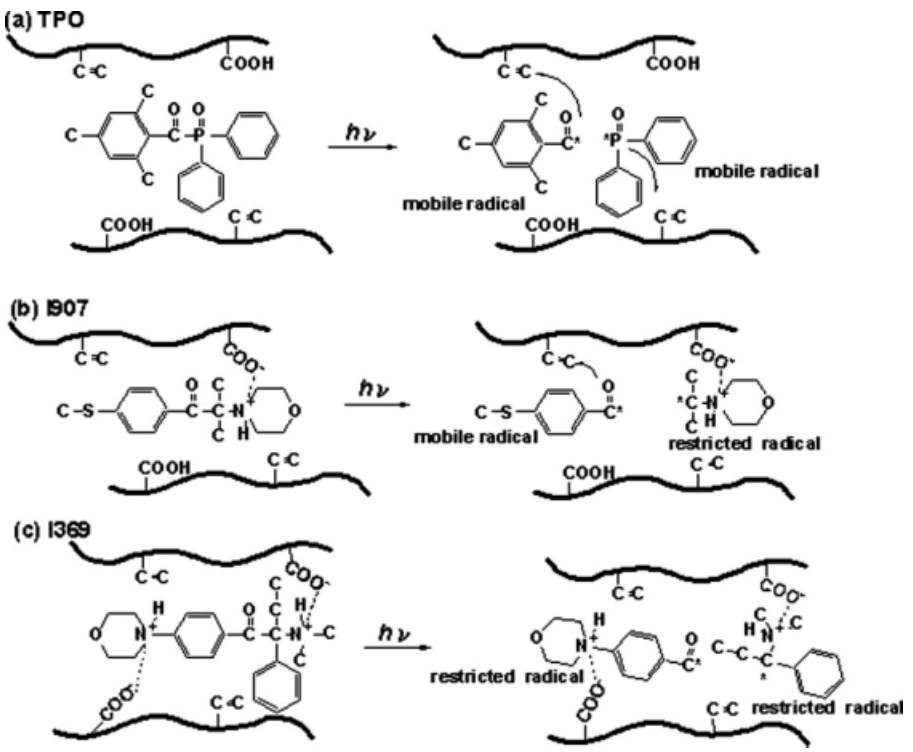

Scheme 2 Interaction between photo-initiators and resins with carboxylic acid group.

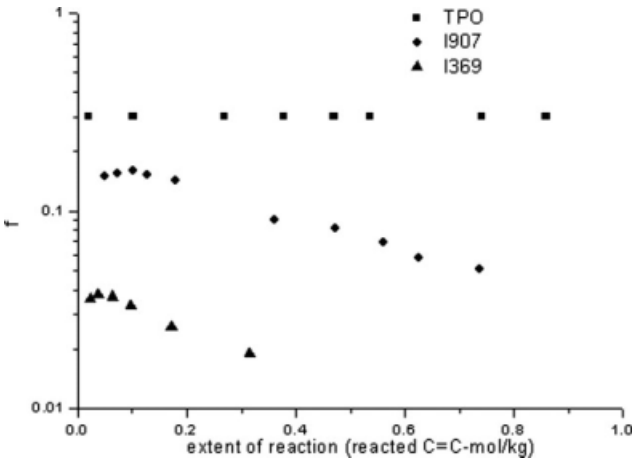

Figure 11 The relationship between f and the extent of reaction for the polymerization of B2 initiated by TPO, I369, and I907, respectively. The fTPO is assumed to be 0.3, and the values of fI369 and fI907 are calculated based on the value of fTPO.

k_t^b, and k_t^m curves of B2 initiated by different PIs are therefore assumed to be the same. After the values of $[P_n^*]$ for I907 and I369 were calculated, f_{I907} and f_{I369} were then calculated by the following equation.

$$f = \frac{[P_n^*]\left(2k_t^b[P_n^*] + k_t^m\right)}{2k_d[I]_0 e^{-k_d t}} \tag{13}$$

where k_t^b and k_t^m values are taken from the curves of B2 shown in Figures 7 and 8, respectively, k_d is the decomposition rate constant of PI, $[I]_0$ is the concentration of PI before UV irradiation, and t is the reaction time during irradiation.

Figure 11 shows the relationship between f and extent of reaction for the polymerization initiated by different PIs. Obviously, f_{I907} and f_{I369} at initial stage of polymerization were smaller than f_{TPO}, especially for f_{I369}. It could be explained by the occurrence of the zwitterionic interaction from the COOH of resin and tertiary amine group of primary radicals, which retarded the mobility and efficiency of the primary radicals. The f_{I369} at initial stage of polymerization was relatively low because both primary radicals produced from I369 contained tertiary amine groups. Compared with I369, a higher f value for I907 at initial stage of polymerization was observed because one of the primary radical, benzoyl radical with a methylthiol group, produced from I907 did not have tertiary amine group and it was still mobile to induce polymerization although the other primary radical, α-aminoalkyl radical, was strongly restricted by zwitterionic interaction. In contrast to I907 and I369, the primary radicals produced from TPO were not restricted by zwitterionic interaction because they did not contain any tertiary amine groups. Therefore, f_{TPO} at initial stage of polymerization was the highest of all.

Figure 11 also shows that the f_{I907} and f_{I369} decreased with extent of reaction, especially for I369. This can be explained by two factors: the increase in viscosity of the reaction medium as reaction proceeded and the restricted mobility of primary radicals by zwitterionic interaction. Therefore, the primary radical produced from PI, especially from I369, was not capable of inducing rapid polymerization of the resin having COOH group.

As mentioned earlier in Figure 9, when using TPO as PI, $[P_n^*]$ increased with extent of reaction due to the reduced k_t^b and k_t^m as the viscosity of reaction medium increased with polymerization. However, this trend was not observed in Figure 12 when using I907 or I369 as PI. Taking I369 for an example, $[P_n^*]$ increased from the beginning of polymerization, reached a maximum, and finally decreased with extent of reaction. It was because the severe drop in f_{I369} over the decrease in k_t^b and k_t^m with extent of reaction. This figure also showed that $[P_n^*]$ decreased in the order of TPO > I907 > I369, which was consistent with the decreasing order of R_p, indicating that the R_p was largely dominated by f of PI. According to this experiment, we can conclude that PI having tertiary amine group is not suitable for initiating the polymerization of resins having COOH group.

CONCLUSIONS

The influence of COOH and amino groups on the photo-polymerization behavior of different kinds of resins was studied. Compared with EPA, it is found that R_p and k_p of resins having COOH, urethane, amide, and imide functional groups are reduced because the mobility of reacting species in the reaction medium is restricted by hydrogen bonding

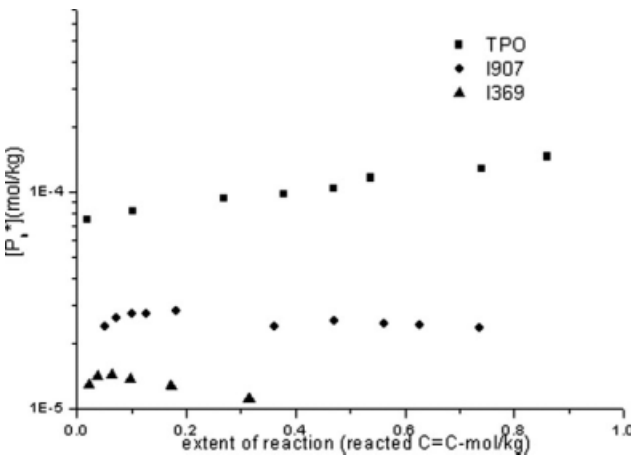

Figure 12 The relationship between $[P_n^*]$ and the extent of reaction of B2 initiated by TPO, I369, and I907, respectively. The intensity of UV light is 1.3 mW/cm^2.

from these functional groups or rigid structure from imide group. Both k_t^b and k_t^m are also reduced by hydrogen bonding, but the largest decreases in k_t^b and k_t^m of resin for B1 are observed because the mobility of growing radicals is strongly restricted by imide group. In addition, it is found that the $[P_n^*]$ of B1 accumulates rapidly and is the largest in all resins used in this study, since the rate of termination in B1 is strongly restricted by imide group. Therefore, R_p of B1 is slightly improved even though its k_p is the lowest of all. Finally, the influence of different PIs, TPO, I907, and I369, on the polymerization was also studied. It is found that the I907 and I369 having tertiary amine group are not suitable for initiating the polymerization of resins having COOH groups because the mobility of primary radicals from PIs and initiator efficiency are largely reduced by the zwitterionic interaction between tertiary amine and COOH groups.

References

1. Luo, N.; Hutchison, J. B.; Anseth, K. S.; Bowman, C. N. Macromolecules 2002, 35, 2487.
2. Lu, H.; Lovell, L. G.; Bowman, C. N. Macromolecules 2001, 34, 8021.
3. Burdick, J. A.; Peterson, A. J.; Anseth, K. S. Biomaterials 2001, 22, 1779.
4. Bosch, P.; Serrano, J.; Mateo, J. L.; Calle, P.; Sieiro, C. J Polym Sci Part A: Polym Chem 1998, 36, 2775.
5. Bosch, P.; Serrano, J.; Mateo, J. L.; Guzman, J.; Calle, P.; Sieiro, C. J Polym Sci Part A: Polym Chem 1998, 36, 2785.
6. Andrzejewska, E.; Zych-Tomkowiak, D.; Bogacki, M. B.; Andrzejewski, M. Macromolecules 2004, 37, 6346.
7. Andrzejewska, E.; Socha, E.; Bogacki, M.; Andrzejewski, M. Polymer 2005, 46, 5437.
8. Mateo, J. L.; Serrano, J.; Bosch, P. Macromolecules 1997, 30, 1285.
9. Lovestead, T. M.; O'brien, A. K.; Bowman, C. N. J Photochem Photobiol A 2003, 159, 135.
10. Kamata, H.; Kamijo, M.; Onishi, M. US Pat. 0041053 A1, 2006.
11. Makita, S.; Kudo, H.; Nishikubo, T. J Polym Sci Part A: Polym Chem 2004, 42, 3697.
12. Lee, C.-H. US Pat. 0175930 A1, 2005.
13. Masson, F.; Decker, C.; Jaworek, T.; Schwalm, R. Prog Org Coat 2000, 39, 115.
14. Cook, W. D. Polymer 1992, 33, 2152.
15. Kuo, K.-H.; Chiu, W.-Y.; Don, T.-M. J Polym Sci Part A: Polym Chem, to appear.
16. Kuo, K.-H.; Chiu, W.-Y.; Hsieh, K.-H.; Don, T.-M. Eur Polym J 2009, 45, 474.
17. Lovell, L. G.; Stansbury, J. W.; Syrpes, D. C.; Bowman, C. N. Macromolecules 1999, 32, 3913.
18. Elliott, J. E.; Lovell, L. G.; Bowman, C. N. Dent Mater 2001, 17, 221.
19. Young, J. S.; Bowman, C. N. Macromolecules 1999, 32, 6073.
20. Rieumont, J. Acta Polym 1986, 37, 422.
21. Deb, P. C.; Ray, S. Eur Polym J 1978, 14, 607.
22. Wen, M.; Mccormick, A. V. Macromolecules 2000, 33, 9247.
23. Brady, G. A.; Halloran, J. W. J Mater Sci 1998, 33, 4551.
24. Cho, J.-D.; Ju, H.-T.; Hong, J.-W. J Polym Sci Part A: Polym Chem 2005, 43, 658.
25. Brandrup, J.; Immergut, E. H. Polymer Handbook, 2nd ed.; Wiley: New York, 1975; p II-425.
26. Odian, G. Principles of Polymerization, 3rd ed.; Wiley: New York, 1991; p 279.
27. Staudt-Bickel, C.; Koros, W. J. J Membr Sci 1999, 155, 145.
28. Chattopadhyay, D. K.; Mishra, A. K.; Sreedhar, B.; Raju, K. V. S. N. Polym Degrad Stab 2006, 91, 1837.
29. Burchell, C. J.; Glidewell, C.; Lough, A. J.; Ferguson, G. Acta Crystallogr Sect B 2001, 57, 201.
30. Wang, Z.; Liu, Q.; Zhu, H.; Liu, H.; Chen, Y.; Yang, M. Carbon 2007, 45, 285.
31. Bressy, C.; Hugues, C.; Bartolomeo, P.; Margaillan, A. Eur Polym J 2003, 39, 319.